Thermal and Dynamic Mechanical Investigations on Fiber-Reinforced Polypropylene Composites

A. AMASH, P. ZUGENMAIER

Institute of Physical Chemistry, Technical University Clausthal, Arnold-Sommerfeld-Str. 4, D-38678 Clausthal-Zellerfeld, Germany

Received April 22, 1996; accepted July 16, 1996

ABSTRACT: The thermal behavior and dynamic mechanical properties of isotactic polypropylene (PP) and reactor blend PP/ethylene–propylene copolymer (EPM), reinforced with different amounts of short glass fibers (GF) and/or polyester fibers (PETF), were investigated by differential scanning calorimetry (DSC) and dynamic mechanical thermoanalysis (DMTA) of imposed tensile load on rectangular film specimens. DSC measurements exhibited an increase of the crystallization temperature of PP in the presence of fibers, but indicated no change in its percentage of crystallinity. DMTA spectra revealed an increase in the stiffness and a decrease of the damping with increasing GF content. The positions of the primary relaxations of PP and EPM did not change, but a significant broadening of the α-relaxation in the crystalline phase was observed, due to the induced reinforcement and interfacial interactions. The addition of PETF to PP enhanced its damping values at low temperatures and promoted the α-transition. The DMTA behavior was studied in dependence on the preconditioning and the frequency excitation. Heat treatment changed the characteristics of the β-relaxation of PP, due to enhanced molecular motion of the polymer segments. The variation of frequency affected the secondary relaxations considerably and, in the presence of GF, the glass transitions. For the different relaxations, activation energies from peak shift and loss peak areas were determined. Experimental data of loss peaks were fitted to phenomenological equations. © 1997 John Wiley & Sons, Inc. J Appl Polym Sci **63:** 1143–1154, 1997

Key words: polypropylene; fiber reinforcement; dynamic mechanical thermoanalysis; relaxation processes

INTRODUCTION

It is well known that the physical properties of a polymeric material are strongly dependent on its morphology, structure, and relaxation processes corresponding to internal changes and molecular motions. In composite materials, the interfacial influence on their properties is also important, in addition to the individual phases of the fibers and the matrix.[1]

Dynamic mechanical measurements over a wide temperature or frequency range are useful in the understanding of the viscoelastic behavior and provide valuable insights into the relationship between structure, morphology, and applicational properties of polymeric and composite materials.[2–6]

In the last years significantly high consumption rates were predicted for polypropylene (PP) and fiber [particularly, glass fiber (GF)] reinforced PP composites, due to the favorable price–performance relationship. Although numerous studies on fiber-reinforced PP composites were reported in literature, fundamental investigations on their structure–property relationships are scarce.[7–9] However, dynamic mechanical thermal investigations of different aspects on film specimens of PP and elastomer-modified PP, reinforced with GF or in addition to polyester fibers (PETF), are less reported or not known to us.

Correspondence to: P. Zugenmaier.

The aim of this work is the study of the thermal and dynamic mechanical behavior of short GF- and/or PETF-reinforced PP composites. The properties of the composites, having a matrix of PP homopolymer and PP/ethylene–propylene copolymer (EPM) blend, are investigated in dependence on temperature, to study the influence of thermal history and frequency variation and to predict a loss modulus curve consisting of different relaxation processes.

EXPERIMENTAL

Materials

Isotactic polypropylene (P5000; MFI = 1.5 g/min; density ρ = 0.902 g/cm^3; $M_w = 263 \cdot 10^3$ g/mol) and a reactor blend iPP/27 wt % EPM (EMV 7184; MFI = 3.7 g/min; ρ = 0.892 g/cm^3; $M_w = 271 \cdot 10^3$ g/mol) were obtained from the HÜLS AG (Marl, Germany). Chopped strands of *E* glass fibers (CP 756; length 4.5 mm and diameter 13 μm), coated with a layer suitable for use with PP, were obtained from the Vetrotex GmbH (Herzogenrath, Germany). One component of this layer is the coupling agent *N*-(aminoethyl)-aminopropyltrimethoxisilane. Chopped strands of PET fibers (Trivera 748; length 6 mm) were obtained from Hoechst AG (Frankfurt, Germany).

Preparation of Composites and Samples

A Haake twin-screw extruder TW100 model (745 mm length × 240 mm diameter) was used for the mixing of both PP types with the short fibers. The temperatures of the four zones of the extruder were 200, 210, 220, and 220°C. The screw speed was adjusted to 40 rpm. The extrudate was cooled in water at room temperature, cut into small granules, and dried for 1 h at 70°C in a vented oven.

For the different measurements presented in this work, films of about 0.3 mm thickness were produced as specimens from the extruded granules, hot-pressed in a hydraulic electrically heated press at 210°C, and then cooled (20°C/min) to room temperature under pressure. The pressing time was 20 min with a force of 50 kN. Some of the samples were obtained by quenching the pressed films to room temperature in a water bath.

MEASUREMENTS

Differential Scanning Calorimetry (DSC)

A DSC-7 (Perkin Elmer) was used for calorimetric studies. A small piece of the film (ca. 10 mg) was used for each experiment. The samples were heated to 180°C and maintained at this temperature for 5 min to eliminate the effects of preconditions. The samples were cooled from 180°C to 25°C at a rate of 10°C/min (cooling cycle), held for 5 min at this temperature, and then heated again to 180°C at a rate of 10°C/min (heating cycle). From the thermograms, transition temperatures and enthalpies can be obtained and the degree of crystallinity determined.

Dynamic Mechanical Thermoanalysis (DMTA)

Stress–strain oscillation measurements were performed at a frequency of 10 Hz with a dynamic mechanical thermoanalyzer, Eplexor of Gabo Qualimeter (Ahlden, Germany), in the linear viscoelastic range using a 15N head. The investigated samples of 30 × 5 mm^2 area and 0.3 mm thickness were cooled to ca. −150°C and heated under a strain-controlled sinusoidal tensile loading to 170°C with a heating rate of 2°C/min in a flow of nitrogen. The static and dynamic strains amount to 0.15% and ±0.05%, respectively. Measurements were taken every 2°C and controlled by Lissajou figure observation on an oscilloscope. The viscoelastic properties, i.e., the complex dynamic modulus (E^*) and the mechanical loss factor (damping) tan $\delta = E''/E'$ (where E'' and E' are loss and storage modulus, respectively), were recorded as a function of temperature. Some measurements were performed over a wide temperature range at different frequencies.

RESULTS AND DISCUSSION

DSC Measurements

The thermal parameters—crystallization temperature (T_c), melting temperature (T_m), heat of fusion (ΔH_f) and the percentage of crystallinity—determined and calculated from the differential scanning thermograms of the considered samples are summarized in Table I. The fiber content is given as wt %. The overall crystallinity (X_c) was determined by using the relationship

Table I Thermal Properties of the Investigated Materials

Material	T_m [°C]	T_c [°C]	ΔH_f [J/g]	X_c/X_c^p [%]
PP homopolymer (PP)	162	112	96.5	50
PP-10%GF	163	113	86	45/45
PP-20%GF	162.5	113.5	79.5	42/40
PP-30%GF	163.5	114	69.5	36.5/35
PP-10%PETF	162	115	87.5	46/45
PP-20%PETF	162.5	116.5	77.5	41/40
PP-10%GF-10%PETF	163.5	116.5	78	41/40
PP-20%GF-10%PETF	162.5	116.5	71	37/35
PP/27%EPM (EMV)	162.5; 116.5	113.5; 99.5	66.5; 3.7	34.5/36.6
EMV-10%GF	162; 116	114; 99.5	60.5; 3.3	32/31.5
EMV-20%GF	161.5	114.5; 99.5	52.5; 3.0	27.5/26.5
EMV-30%GF	161.5	114.5; 99.5	44; 2.8	23/21.5

$$X_c\,(\%\ \text{crystallinity}) = \frac{\Delta H_f}{\Delta H_f^0} \times 100 \qquad (1)$$

A value of ΔH_f^0 190 J/g was taken for 100% crystalline PP homopolymer.[10] The calculated crystallinity (X_c^p) of the polymer composites was obtained by using the additivity equation

$$X_c^p = W_{\text{PP}} \cdot X_{c,\text{PP}} + W_2 \cdot X_{c,2} \qquad (2)$$

with W_{PP} and W_2 the weight fraction of PP and the second component, respectively. Applicability of eq. (2) assumes no interaction between PP and the other crystallizable components.

From the data it is clear that addition of GF and PETF to PP homopolymer causes a slight increase of T_c of the PP matrix. It is remarkable that the influence of the PETF on the crystallization temperature of PP is greater than for pure GF. The observed effect for the incorporation of fibers can be explained by the assumption that the GF and PETF act as nucleating agents, which would increase the crystallization rate of PP.

For the PP–EPM reactor blend (EMV) a small additional crystallization peak of the EPM component is detected and a slightly higher T_c of the PP component compared with neat PP homopolymer is observed. This can be attributed to the enhanced mobility of the PP segments in the presence of EPM, leading to a better alignment in the crystal lattice. The addition of GF to EMV also resulted in a small increase in T_c of the PP component, while the T_c of the EPM component was not affected.

The effect of fibers on the T_m of both PP types is only marginal and indicates no clear tendency. The determined values of ΔH_f and X_c decrease for all investigated samples with increasing GF and PET contents. This is accounted for by the fact that the presence of fibers acts as a diluent in the PP matrix. A comparison of X_c with the calculated X_c^p values shows nearly the same change in the percentage of crystallinity determined by different methods. In general, the overall crystallinity appears to exhibit slightly higher values than the calculated crystallinity, however the observed differences are very low. These results indicate clearly that the incorporation of GF and PETF in the investigated PP types does not affect the crystallization (i.e., crystal growth) of PP considerably. Therefore, the percentage of crystallinity of the PP component remains unchanged in dependence on fiber content.

DMTA Measurements

Storage Modulus and Damping Factor

Some important data representing the dynamic mechanical behavior of the investigated materials are listed in Table II. The temperature dependence of the dynamic mechanical properties is shown in Figures 1–4. The composition of the materials (i.e., the content of the fibers) is given as wt %.

The dynamic mechanical spectra (E' and tan δ as a function of temperature) for the PP homopolymer (PP) and the PP–EPM reactor blend (EMV) are depicted in Figure 1. The tan δ curve of PP exhibits three relaxations located in the vicinity of −80°C (γ), 100°C (α), and at 8°C (β). Their origin has been reviewed by McCrum and colleagues.[11] The γ-peak is due to the relaxing unit consisting of a few chain segments in the

Table II Dynamic–Mechanical Properties of the Materials Investigated at 10 Hz

Material	E′ [MPa]/tan δ at −35°C	E′ [MPa]/tan δ at 23°C	T_g [°C]/tan δ at Peak[a]
PP homopolymer	2750/0.012	1578/0.042	8/0.051 (−80/0.007; 100/0.071)
PP-10%GF	3230/0.012	2100/0.035	8.5/0.044 (109/0.058)
PP-20%GF	3830/0.011	2725/0.027	9.5/0.033
PP-30%GF	4515/0.01	3345/0.022	9.5/0.027
PP-10%PETF	2774/0.014	1697/0.039	9/0.047
PP-20%PETF	3062/0.016	1834/0.035	9/0.045 (−77/0.011; 108/0.082)
PP-10%GF-10%PETF	3400/0.013	2317/0.03	8/0.038
PP-20%GF-10%PETF	4180/0.012	2838/0.028	8.5/0.035
PP/30%EPM (EMV)	1796/0.03	830/0.051	PP: 9.5/0.062 (100/0.082) EPM: −48/0.049 (−123/0.015)
EMV-10%GF	2223/0.028	1215/0.047	9.5/0.054; −48/0.041
EMV-20%GF	2704/0.024	1620/0.042	10/0.048 (112/0.054) −48.5/0.037 (−123/0.015)
EMV-30%GF	3133/0.02	2068/0.036	10.5/0.04; −48.5/0.028

[a] Secondary relaxations in parentheses: T [°C]/tan δ.

amorphous regions. The dominant β-relaxation corresponds to the glass–rubber transition of the amorphous portions and the temperature of the peak maximum is assigned to glass temperature (T_g). For this dispersion a slight rubbery plateau of the stiffness (E') can be observed between T_g and T_m. The small α-relaxation peak appears as a shoulder and can be attributed to a lamellar slip

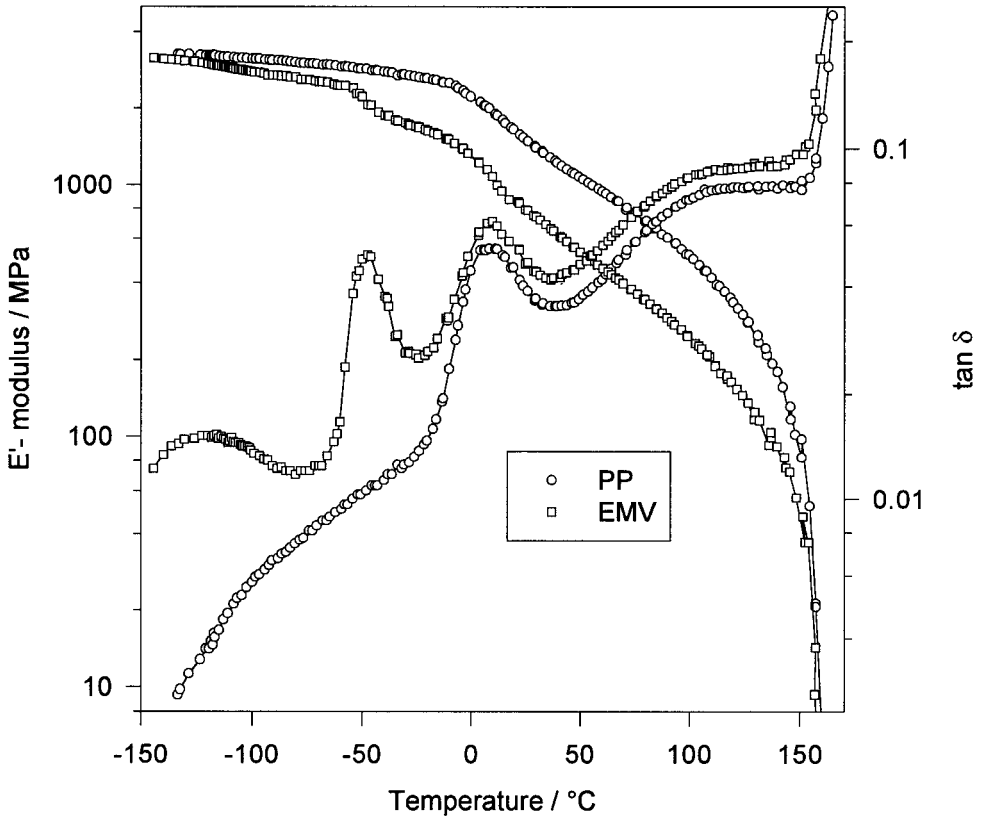

Figure 1 E' and tan δ (DMTA spectrum) of neat PP and PP/27 wt % EPM blend (EMV) as a function of temperature.

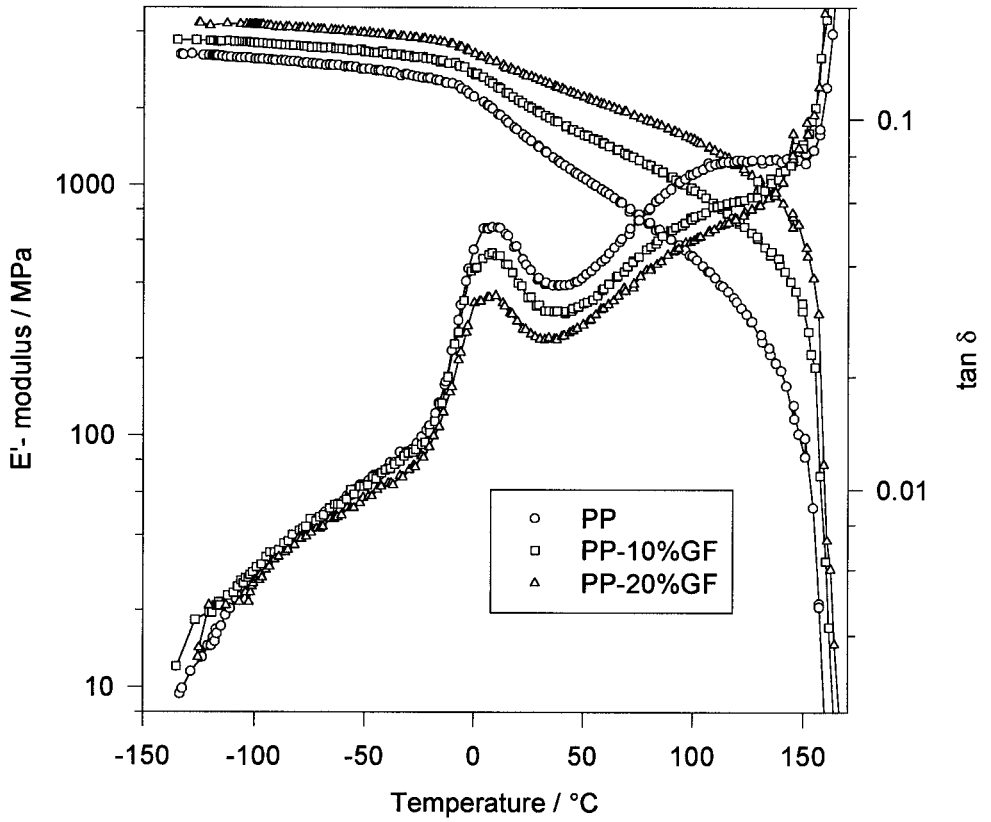

Figure 2 Effect of GF reinforcement on the DMTA spectrum of PP.

mechanism and rotation in the crystalline phase. In the PP–EPM blend, several clear relaxation regions were observed. The detected peaks at 100°C and 8°C belong to the PP component as explained previously. The main or primary relaxation of the EPM component is caused by a glass transition of this amorphous rubber, with the tan δ peak maximum located at $T_g = -48$°C. At lower temperatures (ca. −123°C) the elastomer displays a broad relaxation, which can be attributed to the local rotary motion of long ethylene sequences, similar to that observed in PE.[11] Below 0°C EMV exhibits considerably higher tan δ values corresponding to a higher impact strength and toughness, as compared with PP. However, in the PP-27% EPM blend under investigation, the T_g of the PP component remained nearly unaffected compared with T_g of neat PP homopolymer. This indicates that EMV is an incompatible system consisting of two phases. At very low temperatures the stiffness of EMV is comparable to that of PP, but with temperature increasing the E' modulus curve (Fig. 1) indicates a significant decrease at the T_g of the EPM and PP components.

Figure 2 depicts the DMTA spectra of two PP–GF composites with different compositions. Compared to the DMTA spectrum of neat PP, the characteristics of the DMTA behavior of these composites may be summarized as follows:

1. The incorporation of short glass fibers in PP results in a considerably enhanced stiffness and heat-form resistance of the produced material, while the tan δ values decrease with increased GF content in a regular manner (see Table II). These mechanical properties depend on the composition of the composites (i.e., volume fraction and individual component properties) and on the adhesion and effectivity of interaction between the fibers and the matrix.
2. The position of the β-relaxation remained nearly unchanged but the peak intensity and magnitude decreased significantly. The constant peak position can be explained by the assumption that the GF do not influence the crystallization or percentage of crystallinity of PP, as shown above.
3. In the α-relaxation region a gradual broadening of the peak shoulder with increased GF content was detected, therefore the relaxation shape and intensity changed con-

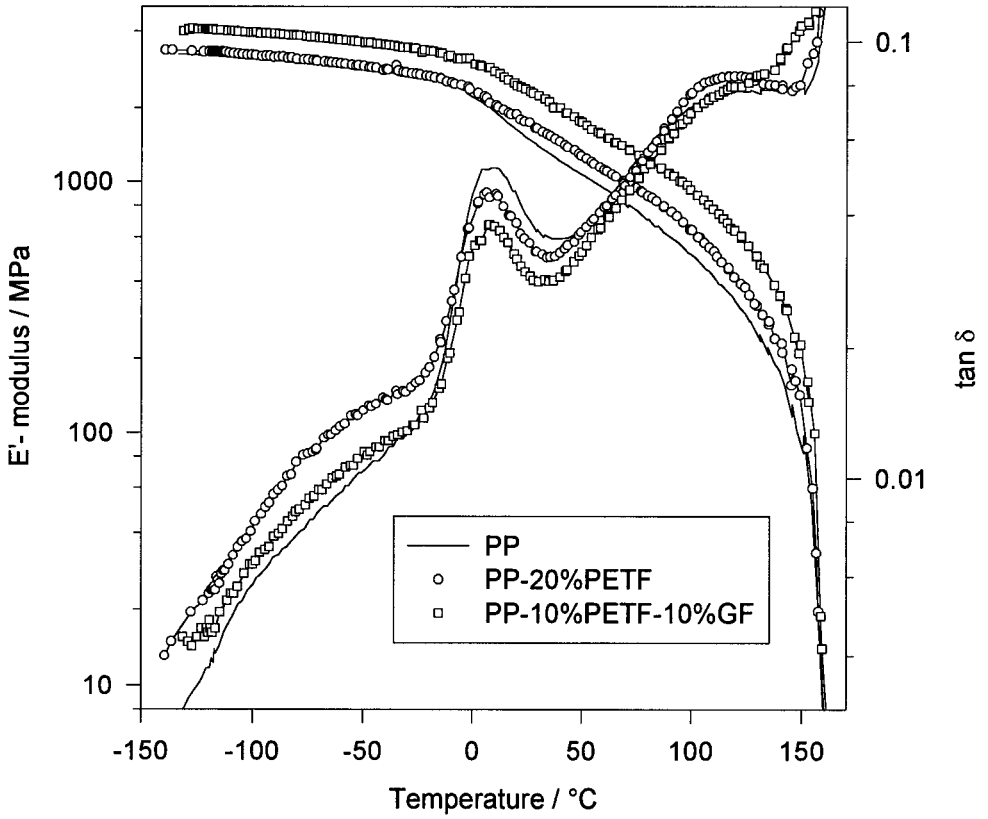

Figure 3 Change in the DMTA traces of PP and PP–GF composite due to PETF addition.

siderably. It seems that the lamellar movement in the crystalline phase is strongly affected by increasing the GF content and consequently, a reinforcement-induced stiffness can be observed. This can be explained by a delay (retardation) of the relative motion of lamellae. Due to their interaction with the GF surface, having a high surface energy, the PP segments become less mobilized and the distribution of their relaxation times is consequently increased. This is confirmed by the loss modulus curves of the same investigated samples.

DMTA spectra for the composites PP–PETF and PP–GF–PETF are depicted in Figure 3. It is remarkable that the addition of 20 wt % PETF to the PP homopolymer enhances the tan δ values at low temperatures (i.e., of γ-relaxation), reduces the magnitude of the T_g peak and promotes slightly the appearance of the α-relaxation above room temperature. These observations can be explained by the presence of interactions in an interphase of matrix and fiber, leading to facilitation of the molecular motion of PP segments. Another explanation may be found in an overlapping of different relaxations (mainly α and γ) which occur in the same temperature range and correspond to segment motion of PP and PET, respectively. By DSC measurements of used short PETF a melting peak only at 260°C could clearly be detected. However, it is noteworthy that the appearance of additional relaxations or enhanced damping values below the T_g of the matrix would improve the toughness and impact strength of the material.[12] The influence of the PETF incorporation on the stiffness was very slight. For the composite PP–GF–PETF, in comparison with PP–PETF, reduced damping values and enhanced E' modulus were observed. The α-relaxation was again affected, i.e., it became broader.

In Figure 4, compared with the PP–EPM blend, DMTA data are summarized for the composite EMV–GF. In addition to the changes explained above for the composite PP–GF, the relaxations of the EPM component (with respect to position and shape) were changed considerably (see also Table II). However, the intensity and magnitude of the different observed peaks, mainly at the lower temperatures, decreased with in-

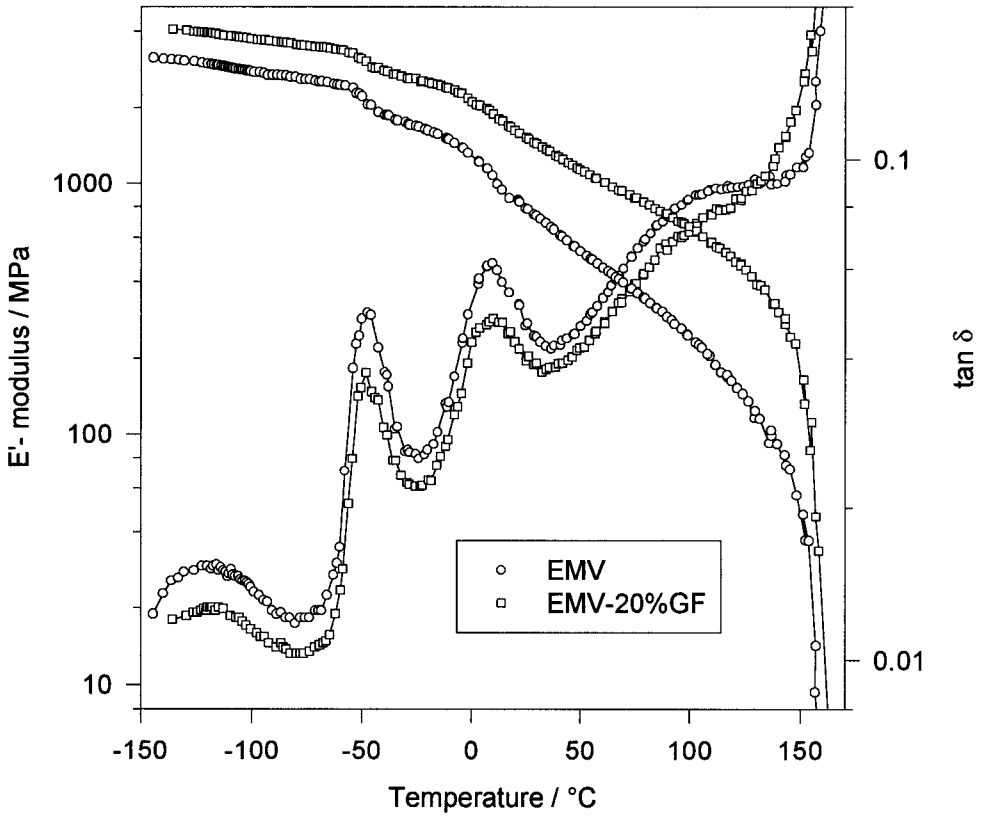

Figure 4 Effect of GF reinforcement on the DMTA spectrum of EMV.

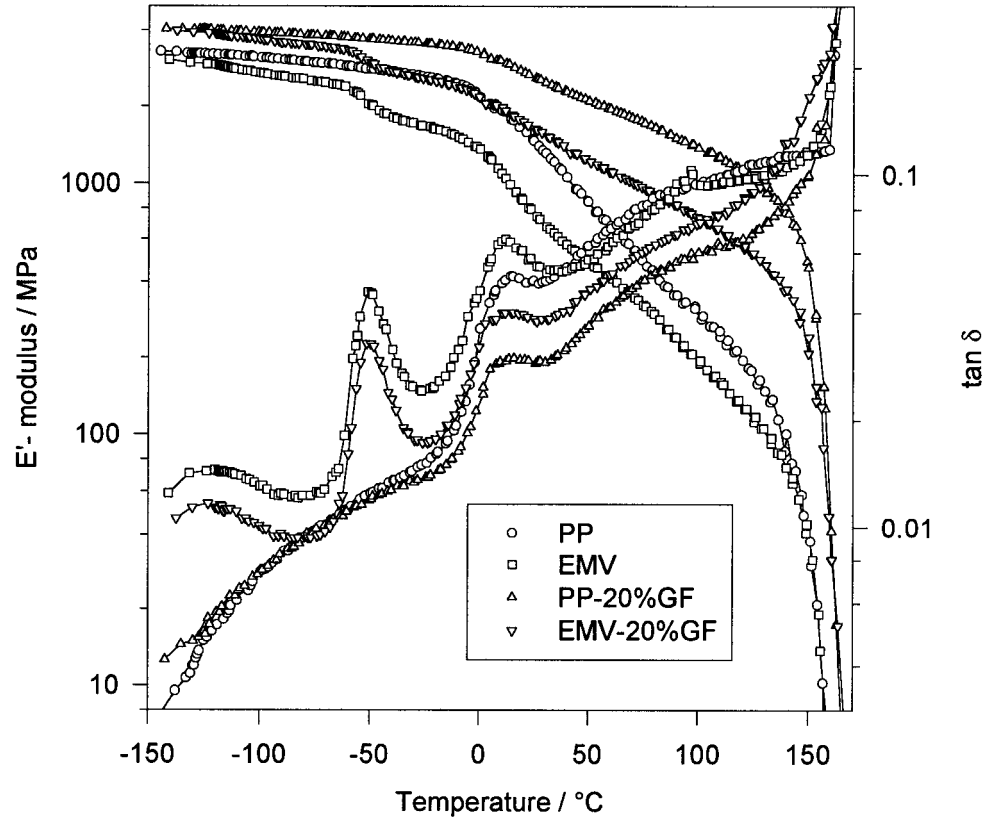

Figure 5 E' and tan δ of rapidly quenched PP, EMV, PP–GF, and EMV–GF composites as a function of temperature.

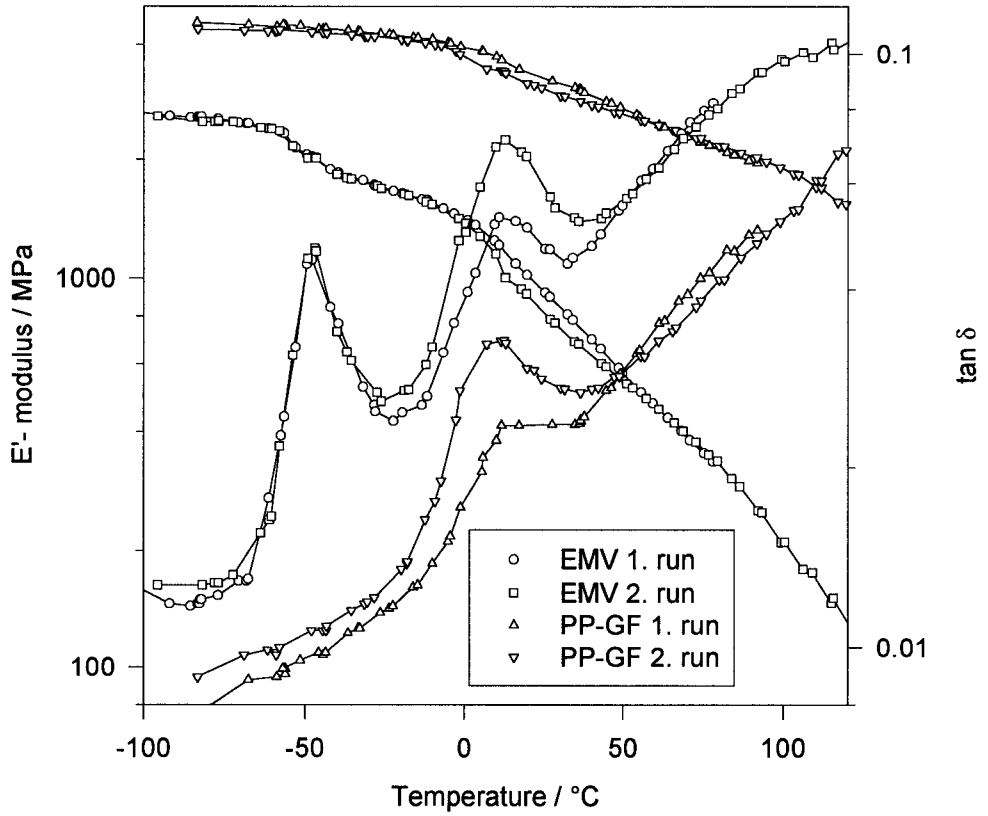

Figure 6 Effect of thermal history (mechanical heat treatment) on DMTA spectra of EMV and PP–GF composite.

creasing GF content but it seems that the molecular motion in the EPM component was not hindered. Furthermore, the stiffness decrease of EMV at the T_g of EPM remained recognizable in the presence of GF, while a relatively slighter one at T_g of the PP component was now detected. The advantage of this composite is its high toughness at low temperatures and improved stiffness above the T_g of PP. This was confirmed for the composite EMV-20 wt % GF by standard measurements (DIN) of stress–strain and impact toughness, which yielded values of 1800 N/mm^2 and 15 mJ/mm^2, respectively.

Effects of Thermal History

The DMTA behavior of the investigated PP types and their composites can be affected significantly by rapid quenching of the produced samples. In Figure 5, DMTA spectra are shown for rapidly quenched samples of PP, EMV, and their composites with 20 wt % GF. Passaliga and Martin[13] have studied some aspects of the influence of thermal history on the relaxation behavior of PP. Compared with the DMTA data in Figure 1, the tan δ curve of rapidly quenched iPP exhibits a broader β peak and T_g is shifted to 14°C. The tan δ values above the T_g are considerably higher, while the stiffness is slightly decreased and the α-relaxation becomes less pronounced since it depends on the crystal morphology.[11] Therefore, the observed changes can be attributed to the decreased degree of crystallinity and poorly developed crystals. For rapidly quenched samples of PP–GF composites, it is noticeable that the β relaxation appears more or less as a stage with nearly the same tan δ maximum value over a temperature range of ca. 10°C, leading to a partial overlapping of the α- and β-relaxation regions. The DMTA spectra of rapidly quenched EMV and EMV–GF composite exhibit nearly the same relative changes as observed for PP and PP–GF, respectively. The remarkable influence of rapid quenching on the T_g of PP in the presence of GF may be attributed to the increased effectivity of adhesion in the interface of GF and the PP matrix. This can be confirmed by considering the significant increase of stiffness (i.e., well-developed rubbery plateau) induced by GF incorporation. An explanation can be found by different stresses in

the composite (mainly mechanical stress in the interface area) being frozen by rapid quenching and acting as improved reinforcement effects.

The influence of the thermal history on the DMTA behavior was studied by considering the effect of heat treatment combined with tensile load. The same sample produced by quenching was measured in a first run in the DMTA from −100 to 100°C, and later loaded in a time sweep under a low dynamical tension (strain amplitude ±0.05%) for 30 min, subsequently cooled to −100°C without reclamping, and again heated to the melting point. As an example, Figure 6 depicts the results of both heating cycles for the neat reactor blend PP–EPM and the composite PP–GF. The tan δ curves determined by a second run exhibit a remarkable change in the region of the T_g of PP matrix (in EMV PP component) as compared with the corresponding curves of the first run. The shape, intensity, and position of the considered β-relaxation were affected by prior treatment. The significant increase of damping, corresponding to a relative reduction of the E'-modulus in the glass transition region, may indicate a greater or improved molecular motion of PP chains in the amorphous regions. Therefore, a further significant crystallization in PP during the first heat treatment and time sweep would not be assumed in this case. The enhanced segment mobility may arise from a change in the polymer's molecular alignment due to the prior treatment and leading to a facility of chain movement at the corresponding imposed frequency. Moreover, it can be assumed that entanglements and different frozen stresses, which act as network points and reinforcement effects, would ease off considerably due to the thermal-mechanical treatment and probably arising from microrips in the PP-GF composite. For the neat PP-EPM blend, it is noteworthy that the T_g (i.e., with respect to shape, magnitude, and position) of the EPM component was not affected by the imposed heat treatment and time sweep. This can be attributed to the high elasticity and noncrystallinity of the molecular chains of the considered elastomer. In the presence of GF the main relaxation of EPM changed slightly in the second DMTA run, probably because of the influence of prior treatment on adhesion interaction as explained previously.

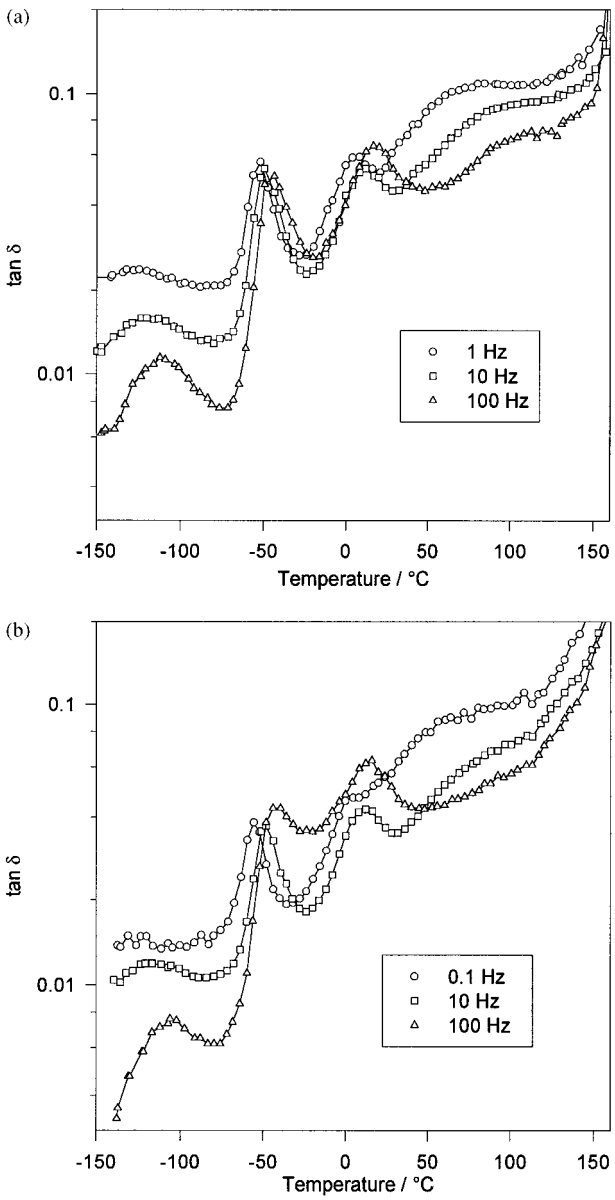

Figure 7 (a) Tan δ of EMV as a function of temperature at various frequencies. (b) Tan δ of EMV-20% GF as a function of temperature at various frequencies.

Effects of Frequency

The DMTA data of several materials investigated have been determined over a temperature range of −150°C to 150°C at four frequencies (0.1, 1, 10, and 100 Hz). In Figure 7(a) the temperature dependence of tan δ is depicted for the PP-EPM blend (EMV) at three frequencies. The secondary relaxation of the EPM component was very strongly affected by increasing the frequency of measurement. The peak became gradually narrower, the magnitude decreased significantly and a great increase in the relaxation temperature was detected from −145 (for 0.1 Hz) to −112°C (for 100 Hz). The effect of frequency on relaxations corresponding to the glass transitions of the EPM and PP components was less pro-

Table III Activation Energies from Peak Shifts and Loss Peak Areas

Material	Relaxation Process	ΔE_a Shifts (kJ/mol)	ΔE_a Peak Areas (kJ/mol)
PP homopolymer	α	158	
	β	364	358
PP-20%GF	β	355	330
PP-20%PETF	α	160	
	β	363	360
PP/27%EPM (EMV)	β_{PP}	359	350
	α_{EPM}	248.5	246
	β_{EPM}	38	36.5
EMV-20%GF	β_{PP}	353	331.5
	α_{EPM}	242	236
	β_{EPM}	34	33.5

nounced. However, the relaxation temperatures of both components also increased by about 10°C with frequency from 0.1 to 100 Hz. The T_g of PP indicated a change from 8 to 17°C and for EPM from −52 to −43°C. A remarkable influence of frequency was observed for the α-relaxation of PP, which occurs in the crystalline phase. The frequency increase reduced the intensity (i.e., tan δ values) and shifted the position of the relaxation region to higher temperatures. The peak became broader and less pronounced, due to the additional melting region at higher temperatures. By varying the measurement frequency, the DMTA behavior of EMV was much more influenced in the presence of GF (Fig. 7b). Certainly, the greatest effect was observed at a frequency of 100 Hz, which changed the tan δ curve considerably. For addition of GF the character of the EPM β-relaxation, explained previously for neat EMV, was significantly affected by imposing a frequency of 100 Hz. Moreover, the tan δ curve exhibits increased values over a wide temperature range from about −50°C to 20°C and a significant overlap of the T_g peaks of the PP and EPM components. It can be assumed that a further frequency increase would lead to a complete overlapping of the considered relaxations. For other samples (PP, PP–GF and PP–PETF) investigated under the same conditions, similar results were obtained. Because the PETF promotes the appearance of the α-relaxation in crystalline phase, a pronounced α-peak could be detected, mainly at low frequencies.

The relationship between the temperature at which a relaxation process is observed (T) and the frequency of excitation (f) can be given by the Arrhenius equation[14]:

$$f = f_0 \cdot \exp \frac{-\Delta E_a}{RT} \qquad (3)$$

where f_0 is a constant, R is the gas constant (8,314 $JK^{-1}\,mol^{-1}$) and ΔE_a is the activation energy for the relaxation. This can be derived from loss peak positions T_1 and T_2 at two frequencies, f_1 and f_2, given in

$$\log\left(\frac{f_1}{f_2}\right) = \frac{\Delta E_a}{2.303R} \cdot \left(\frac{1}{T_1} - \frac{1}{T_2}\right) \qquad (4)$$

Calculated activation energies according to eq. (4) are summarized in Table III for some of the samples investigated. In all thermoplastics the greatest ΔE_a value was determined for the glass transition of PP. The secondary relaxation of the EPM component yielded the lowest activation energy. The presence of GF slightly decreased the different activation energies, whereas the PETF did not affect the ΔE_a values of PP relaxations.

Read and Williams[15] have shown that from a plot of the loss modulus (which is correlated to the loss factor) versus the inverse temperature, the area below the loss peak allows the determination of the average activation energy, given by the relationship[15]:

$$\Delta E_a = \left\langle \frac{1}{\Delta E_a} \right\rangle^{-1} = (E_u - E_r) \cdot \frac{R\pi}{2} \cdot \frac{1}{\int E'' d\left(\frac{1}{T}\right)} \qquad (5)$$

where $(E_u - E_r)$ is the relaxation strength and u and r denote the unrelaxed and relaxed states of the sample, respectively.

A comparison of values determined from eqs.

(4) and (5) is given in Table III. Values of the activation energy calculated from loss peak areas are lower than the corresponding values from an Arrhenius relationship, but exhibit a similar tendency.

Prediction of the E″ *Modulus*

The temperature dependence of a single relaxation peak can be described by the following relationship[16]:

$$E''(T) = E''_{\max} \cdot \frac{1}{\cosh\left[a \cdot \frac{\Delta E_a}{R} \left(\frac{1}{T} - \frac{1}{T_{\max}} \right) \right]} \quad (6)$$

where a is a parameter for the half-width of the loss modulus ($0 < a < 1$) and $T_{\max}$ is the temperature at which E'' reaches a maximum ($E''_{\max}$). It is noteworthy that an analogous relationship is given for the dielectric relaxation known as the Fouss–Kirkwood equation.[11]

In Figure 8(a) the loss modulus of EMV–GF composite is depicted versus the inverse temperature. The curve consists of different relaxation regions corresponding to EPM and PP with a contribution of GF, as explained above. By the application of eq. (6) the individual relaxation peaks of the observed loss modulus curve were fitted [Fig. 8(a)]. Unfortunately, the predicted E'' values exhibit a considerable deviation from the experimental results, particularly at the ends of the peaks. Therefore, it can be assumed that the equation for the prediction of the loss modulus should include a term which considers the skewedness and the partial overlap of the different relaxation peaks. Accordingly, an exponent as a damping factor was inserted in eq. (6), leading to the relationship

$$E''(T) = E''_{\max} \cdot \frac{1}{\cosh\left[a \cdot \frac{\Delta E_a}{R} \left(\frac{1}{T} - \frac{1}{T_{\max}} \right) \right]^m} \quad (7)$$

with

$$m = m_0 + \frac{T_{\max}}{T}$$

The results predicted by using eq. (7) are shown in Figure 8(b). A physical interpretation of m cannot be given at this time. It is clear that the modified equation more suitably fits the experimental data and describes the temperature dependence of the relaxation peaks.

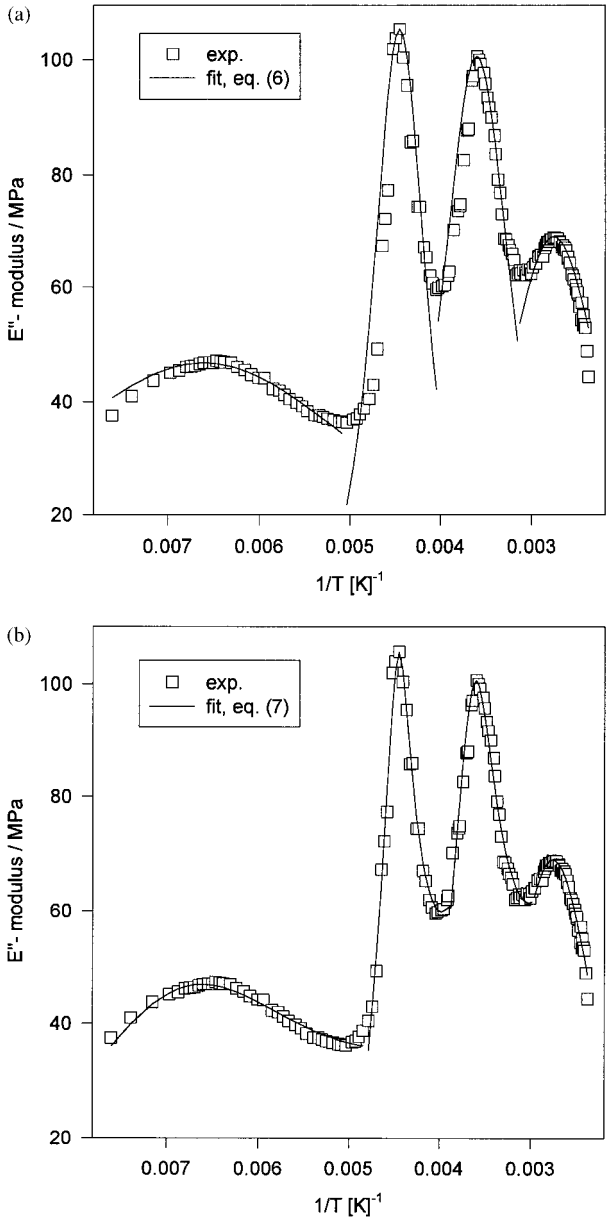

Figure 8 (a) Fitted E'' peaks of EMV–GF composite via eq. (6). (b) Fitted E'' peaks of EMV–GF composite via eq. (7).

CONCLUSIONS

1. DSC thermograms indicate that the addition of GF and PETF to PP or EMV causes an increase in the rate of crystallization. Since the added fibers do not affect the

crystal growth, no significant change in the percentage of crystallinity of PP was observed.

2. The incorporation of GF and/or PETF in both polymeric materials under investigation affects their viscoelastic behavior considerably, due to reinforcement effects and interactions in the interphase area of fiber and matrix. With increasing GF content the E' modulus increases and tan δ decreases in a regular manner. The positions of the relaxations in the amorphous regions do not change but the relaxation in the crystalline phase is strongly affected. The presence of PETF enhances the damping values of PP at low temperatures.
3. The procedure of preconditioning affects the DMTA properties of the investigated samples considerably. The effectivity of interfacial adhesion of GF and PP matrix is also dependent on the thermal history.
4. The variation of excitation frequency affects the secondary relaxations of the investigated polymers significantly. In the presence of GF, this effect can also be found for the primary relaxations.

REFERENCES

1. P. K. Sengupta and D. Mukopadhyay, *J. Appl. Polym. Sci.,* **51,** 831 (1994).
2. I. M. Ward, *Mechanical Properties of Solid Polymers,* Wiley Interscience, London, 1971.
3. T. Murayama, *Dynamic Mechanical Analysis of Polymeric Material,* Elsevier, Amsterdam, 1978.
4. S. Poltersdorf, B. Poltersdorf, W. Schlüter, and V. F. Gaddum, *Kunststoffe,* **80,** 1283 (1990).
5. B. F. Read and G. D. Dean, *The Determination of Dynamic Properties of Polymers & Composites,* Wiley, New York, 1978.
6. L. E. Nielsen, *Mechanical Properties of Polymers & Composites,* Marcel Dekker, New York, 1975.
7. R. Schledjewski and J. Karger-Kocsis, *J. Thermoplast. Compos. Mater.,* **7,** 270 (1994).
8. J. I. Kroschwitz, Ed., *Encyclopedia of Polymer Science & Engineering,* 2nd ed., Vol. 5, Wiley, New York, 1989, p. 300.
9. J. M. Felix and P. Gatenholm, *J. Appl. Polym. Sci.,* **50,** 699 (1993).
10. S. Lohnmayer, *Die speziellen Eigenschaften der Kunststoffe,* Expert Verlag, Gafenau, 1984.
11. N. G. McCrum, B. E. Read, and G. Williams, *Anelastic and Dielectric Effects in Polymeric Solids,* John Wiley and Sons, London, 1967.
12. F. Ramsteiner, *Kunststoffe,* **73,** 148 (1983).
13. E. Passaliga and G. M. Martin, *J. Res. Nat. Bur. Stds.,* **68A,** 519 (1964).
14. J. Heijboar, in *Molecular Basis of Transitions and Relaxations,* D. J. Meier, Ed., Gordon and Breach Science Publishers, New York, 1978, p. 75.
15. B. E. Read and G. Williams, *Trans Faraday Soc.,* **57,** 1979 (1961).
16. C. A. F. Tuijnman, *J. Polym. Sci.,* **C16,** 2379 (1967).